The charge-effect transistor

M. Amman and K. Mullen
Department of Physics, The University of Michigan, Ann Arbor, Michigan 48109

E. Ben-Jacob
Department of Physics, The University of Michigan, Ann Arbor, Michigan 48109, and School of Physics and Astronomy, Raymond and Beverly Sackler Faculty of Exact Sciences, Tel-Aviv University, 69978 Tel-Aviv, Israel

(Received 29 April 1988; accepted for publication 18 August 1988)

We present a theoretical study of the current-voltage characteristic of a new transistor based upon the "Coulomb blockade." In mesoscopic (submicron) tunnel junctions the flow of current can be blocked by the electrostatic charging energy of a single electron. The charge-effect transistor is composed of two mesoscopic tunnel junctions connected in series with a gate terminal capacitively coupled to the interjunction region. Such a device has been shown to lead to a Coulomb staircase in the current-voltage characteristic when the gate voltage is zero. Here we study the effect of the gate voltage on the current through the device for various ranges of junction parameters. We study junctions made from both normal metal and superconductors. We examine the current noise at different operating points and find it comparable to, but lower than, that in ordinary shot-noise devices.

I. INTRODUCTION

Modern device fabrication techniques have made it possible to construct tunnel junction devices on the submicron level.[1] Such mesoscopic devices are the next step in the evolution of small devices whose primary objectives are faster characteristic device times and lower dissipation. New effects arise in this mesoscopic domain as a result of the quantum mechanical phase of the electron, as well as the discrete nature of the electronic charge.[2] Among the new effects predicted are oscillations in the voltage across a mesoscopic tunnel junction when it is driven by a current source of magnitude I_{dc}. It is predicted that a normal (nonsuperconducting) mesoscopic junction of capacitance C will exhibit voltage oscillations of amplitude $e/2C$ and frequency I_{dc}/e.[3–16] In addition, a voltage shift of $e/2C$ in the I-V characteristic for such a configuration has been predicted and experimentally verified.[17,18] The configuration of two mesoscopic junctions coupled in series and driven by a voltage source has also been considered. Such a system is also predicted to show an offset from the normal ohmic result as a result of electrostatic charging energy[19,20] and, for certain junction parameters, can display steps in the I-V characteristics.[20] The offset and steps have been observed in ensembles of such junctions[21–23] as well as in single junctions formed lithographically[24] or from a scanning tunneling microscope.[25]

In this paper we analyze a three-terminal mesoscopic device: two serially coupled mesoscopic junctions driven by a voltage source as shown in Fig. 1. A three-terminal device is more useful than a two-terminal device in that the former is applicable to such functions as signal amplification, logic operations, and memory. The basic principle involved is the control of the device current by means of the application of a small control signal. A switch is thus obtained in the extreme case where the small signal can cause the device current to change from zero to a large value. We consider junctions made from normal or superconducting materials. In the latter case we assume that the resistances are large so that the Josephson coupling energy, $E_J = \pi\hbar\Delta(T)/2e^2R$, where $\Delta(T)$ is the superconducting coupling energy,[26] is smaller than kT so that the Josephson current is negligible. Alternatively, junction parameters can be chosen so that $\Delta(T) < e^2/2C$, thus reducing the pair current.[27] We neglect the possibility of incoherent pair tunneling.[28] We assume that the dc voltage source, having zero internal resistance, holds the potential across the coupled junctions at a constant value V_{dc}. The voltage source V_{ex}, coupled capacitively to the interjunction region, acts to apply a small signal charge $Q_{ex} = C_{ex}V_{ex}/e$ to the interjunction region, where Q_{ex} is a continuous variable measured in units of e. The tunnel junction device utilized in this circuit is a transistorlike device controlled through charge variations in the interjunction region, hence the name charge-effect transistor (CHET).

In Sec. II we apply the semiclassical picture to the CHET circuit in order to predict its dynamical behavior. The dynamics are expressed as a stochastic process for N, the number of extra interjunction electrons. A master equa-

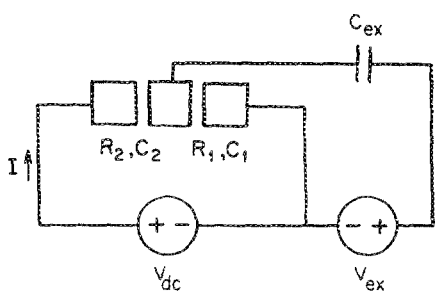

FIG. 1. Schematic representation of two mesoscopic tunnel junctions connected in series, driven by the voltage source V_{dc} and controlled by the voltage source V_{ex}.

 0021-8979/89/010339-08$02.40

tion[29] for the probability distribution of N is obtained from the stochastic process, allowing the calculation of device characteristics. Some of the assumptions implicit in such an approach are detailed at the end of the section.

Numerically calculated circuit characteristics for normal-metal junctions of various parameters are then presented in Sec. III. We find that by varying Q_{ex} for fixed V_{dc} we can control the current through the device. The exact form of the I-V characteristic depends upon the relative RC times of the two junctions constituting the transistor, but is always periodic in Q_{ex}. We calculate the power spectrum of the current noise and find it comparable to, but lower than, that of shot-noise devices. This is in agreement with Ref. 30 where it is shown that the electrostatic charging energy can reduce the noise.

In Sec. IV we calculate the I-V characteristics of CHETs made from superconducting materials. By using superconductors we introduce a new energy scale, that of the superconducting energy gap. We find that in this case the nonlinearity of the transistor is enhanced so that the switching characteristics of the device are made more sharp.

We conclude in Sec. V by discussing our results and suggesting ways in which they might be extended to other systems.

II. THE SEMICLASSICAL MODEL FOR CHARGE-EFFECT TRANSISTORS

We theoretically analyze the CHET circuit through the use of the semiclassical model.[5,7,11] The basic view in this model is that the state of each junction is described by a single classical variable, the voltage across the junction. The voltage across each junction for fixed V_{dc} and V_{ex} is determined, in turn, by N, the number of surplus electrons in the interjunction region. The time evolution of the system is then described by a stochastic process composed of a series of single-electron tunneling events that alter N. To simplify the presentation of the model for the CHET circuit, the case of a zero-signal charge ($Q_{ex}=0$) will be considered first. The stochastic process is then given by[20]

$$N(t+\Delta t)=\begin{cases} N(t)+1, & \text{with probability } [r_1(V_1)+l_2(V_2)]\Delta t, \\ N(t)-1, & \text{with probability } [r_2(V_2)+l_1(V_1)]\Delta t, \\ N(t), & \text{with probability } 1-[r_1(V_1)+l_1(V_1) \\ & \quad +r_2(V_2)+l_2(V_2)]\Delta t, \end{cases} \tag{1}$$

where $r_i(V_i)$ and $l_i(V_i)$ are the instantaneous rates of an electron tunneling from the right and left, respectively, and the subscript i refers to the rates and voltages across either the first or second junction. The voltages across each junction are

$$V_1=V_{dc}\frac{C_2}{C_1+C_2}-\frac{Ne}{C_1+C_2},$$
$$V_2=V_{dc}\frac{C_1}{C_1+C_2}+\frac{Ne}{C_1+C_2}, \tag{2}$$

where it has been assumed that the relaxation time in each electrode is much shorter than the electron tunneling time. The stochastic process (1) states that the probability of N increasing by one in a time interval Δt is the sum of the two rates that increase the charge in the interjunction region multiplied by Δt, and similarly for N decreasing by one. The probability that N remains constant is the remainder. We assume the resistances are large enough ($R>\hbar/e^2$) so that electrons are localized on one side of the junction or the other, thus restricting N to integral values.

To see how the transition rates depend upon the junction voltages, we calculate $r_1(V_1)$, noting that the other rates can be similarly defined. If $T(E)$ is the tunneling matrix element for an electron in a state of energy E and if we assume that the quantum probabilities for elastic tunneling of electrons in different energy levels are independent, then the net transition rate is calculated by integrating over the single-electron energy levels[31]:

$$r_1(V_1)=\int_{-\infty}^{\infty}\frac{2\pi}{\hbar}|T(E)|^2 D_m(E-E_m)D_r(E-E_r) \times f(E-E_r)[1-f(E-E_m)]dE, \tag{3}$$

where $f(E)$ is the Fermi distribution function, $D_m(E)$ and $D_r(E)$ are the density of states for the middle and right sections of the coupled junctions, and similarly E_m and E_r are their Fermi energies. For junctions made from normal metals, $D_m(E)$, $D_r(E)$, and $|T(E)|^2$ are assumed to be energy independent, so that $D_m(E)=D_{m0}$, $D_r(E)=D_{r0}$, and $|T(E)|^2=|T_0|^2$. The integral (3) then simplifies to a dependence on the overlap of $f(E-E_r)$ and $1-f(E-E_m)$, and thus depends on $\Delta E_1(N)\equiv E_m-E_r$, the energy an electron gains in tunneling across the first junction. This change in energy is

$$\Delta E_1(N)=e\int_N^{N+1}V_1(N')dN'=eV_1-\frac{e^2}{2(C_1+C_2)}, \tag{4}$$

where eV_1 is energy supplied by the voltage source and $-e^2/2(C_1+C_2)$ is electrostatic energy transferred from the junction to the tunneling electron. Similarly, for the second junction, $\Delta E_2(N+1)=eV_2+e^2/2(C_1+C_2)$. Note that $\Delta E_1(N)+\Delta E_2(N+1)=eV_{dc}$, which is the gain in energy of an electron in traveling through the device. In Fig. 2(a) we show $r_1(V_1)$ for various temperatures and demonstrate the suppression of tunneling for $V_1<e/2(C_1+C_2)$ when $k_BT<e^2/2C$. For simplicity all subsequent calculations were carried out at zero temperature. This gives the following transition rate for junctions made of normal metals:

$$r_1(V_1)=\begin{cases}\dfrac{\Delta E_1(N)}{e^2R_1}=\dfrac{V_1}{eR_1}-\dfrac{1}{2(C_1+C_2)R_1}, & V_1>\dfrac{e}{2(C_1+C_2)}, \\ 0, \quad \text{otherwise}, \end{cases} \tag{5}$$

where $R_t = \hbar/(2\pi e^2 D_{m0} D_{r0} |T_0|^2)$ is the normal-state resistance of the first junction.

The importance of the magnitude of the resistance can be understood by noting that D_{m0}^{-1} and D_{r0}^{-1} can be interpreted as the separation between single-electron energy levels, and that $|T_0|^2$ is proportional to the square of the overlap energy of the single-electron energy levels on either side of the junction. When $R_t > \hbar/2\pi e^2$, then $D_{m0}^{-1} D_{r0}^{-1} > |T_0|^2$ so that the spacing between levels is greater than their width; this implies that each level can be treated independently so that (3) is valid. When $R_t < \hbar/2\pi e^2$, then $D_{m0}^{-1} D_{r0}^{-1} < |T_0|^2$ and the single-electron energy levels start to overlap so that they can no longer be treated independently.

When the junctions are composed of superconducting materials, interesting dynamical behavior is expected as a result of the discontinuous density of states.[32,33] For this case, assuming Bardeen–Cooper–Schreiffer theory,[34] $r_i(V_i)$ and $l_i(V_i)$ will denote the quasiparticle tunneling rates, and the constant density of states must be replaced by the superconducting density of states:

$$D(E) = \begin{cases} \dfrac{|E - E_f| D_0}{[(E - E_f)^2 - \Delta(T)^2]^{1/2}}, & |E - E_f| > \Delta(T), \\ 0, \quad \text{otherwise}, \end{cases} \tag{6}$$

where E_f is the Fermi energy level, and D_0 corresponds to a constant approximating the density of states for a normal metal. In Fig. 2(b) we show the transition rates for junctions made of superconducting materials. We approximate the superconducting transition rate by

$$r_1(V_1) = \begin{cases} \dfrac{V_1}{eR_1} - \dfrac{1}{2(C_1 + C_2)R_1}, & V_1 > \dfrac{e}{2(C_1 + C_2)} + \dfrac{2\Delta(T)}{e}, \\ 0, \quad \text{otherwise}. \end{cases} \tag{7}$$

The characteristics of the coupled junctions are obtained by iterating the stochastic process (1) for fixed external parameters. This method is useful for obtaining power spectrum or noise information. The ensemble-averaged dynamics of the circuit are more easily obtained from a master equation approach. The stochastic process (1) can be converted to a master equation for $\rho(N,t)$, the probability that there are N electrons in the interjunction region at time t:

$$\begin{aligned} \frac{\partial \rho(N,t)}{\partial t} = {} & [r_1(N-1) + l_2(N-1)]\rho(N-1,t) \\ & + [l_1(N+1) + r_2(N+1)]\rho(N+1,t) \\ & - [r_1(N) + l_1(N) + r_2(N) + l_2(N)]\rho(N,t), \end{aligned} \tag{8}$$

where the transition rates are expressed as functions of N using (2). In order to solve this equation, the initial distribution is assumed to be $\rho(N,t=0) = 1$ for $N = 0$ and $\rho(N,t=0) = 0$ otherwise. The boundary condition for N is $\rho(N = \pm N_{\lim}, t) = 0$, where $N_{\lim}$ is chosen so that $\Sigma_{N=N_{\lim}}^{\infty} \rho(N) < 10^{-5}$. Using these conditions, the stationary distribution $\rho(N)$ is determined from (8), and the average current is calculated by

$$I = \sum_N [r_2(N) - l_2(N)]\rho(N) = \sum_N [r_1(N) - l_1(N)]\rho(N), \tag{9}$$

thus obtaining the dynamics of the circuit.

To externally control the dynamical behavior of the device, we are interested in the case of a nonzero-charge signal. The extension of the model to nonzero Q_{ex} consists of modifying the expressions for the junction voltages:

$$\begin{aligned} V_1 &= V_{dc} \frac{C_2}{C_1 + C_2} - \frac{(N + Q_{ex})e}{C_1 + C_2}, \\ V_2 &= V_{dc} \frac{C_1}{C_1 + C_2} + \frac{(N + Q_{ex})e}{C_1 + C_2}. \end{aligned} \tag{10}$$

With this modification of the junction voltages, the previous dynamical descriptions (1), and (3), and (8) remain valid.

In summary, in order to express the dynamics of the junctions in the semiclassical approach using (1), (3), and (4), we must assume the following[11]: (1) The equilibration rate in the electrodes is much faster than the tunneling rate so that the occupation probabilities of the states are given by the equilibrium Fermi distribution. (2) The phase randomization time is sufficiently short so that multiple tunneling events (repeated tunneling back and forth by a single electron) do not lead to quantum-mechanical interference. (3) The quantum probabilities for the elastic tunneling of electrons of different states are independent. (4) The voltage source V_{dc} delivers charge instantaneously so that the voltage across the device is constant. (5) The resistances of the junctions are large enough ($R > \hbar/e^2$) so that the electrons are localized on one side of the junctions or the other. (6) The capacitances used are the same for all single-electron states and are given by the conventional macroscopic capacitances.

III. NORMAL-METAL CHET

A rich variety of device characteristics are possible with the CHET by varying the junction parameters. In Figs. 3–5 we show examples of theoretically calculated device characteristics, using (8), for the CHET circuit with tunnel junctions made from normal metals. Figures 3(a), 4(a), and 5(a) are graphs of output current I plotted against the dc bias voltage V_{dc} for various signal charges Q_{ex}. Figures 3(b), 4(b), and 5(b), showing I-Q_{ex} for various V_{dc}, are the transfer characteristics of the device, which are an alternate presentation of the same data.

In Fig. 3 we assume that the resistances and capacitances of the two junctions are equal. In this case the current scales with $1/RC$ and the voltage scales with $1/C$, where $R = R_1 = R_2$ and $C = C_1 = C_2$. First note that for $Q_{ex} = 0$, when $V_{dc} < e/2C$, the current is suppressed as a result of the

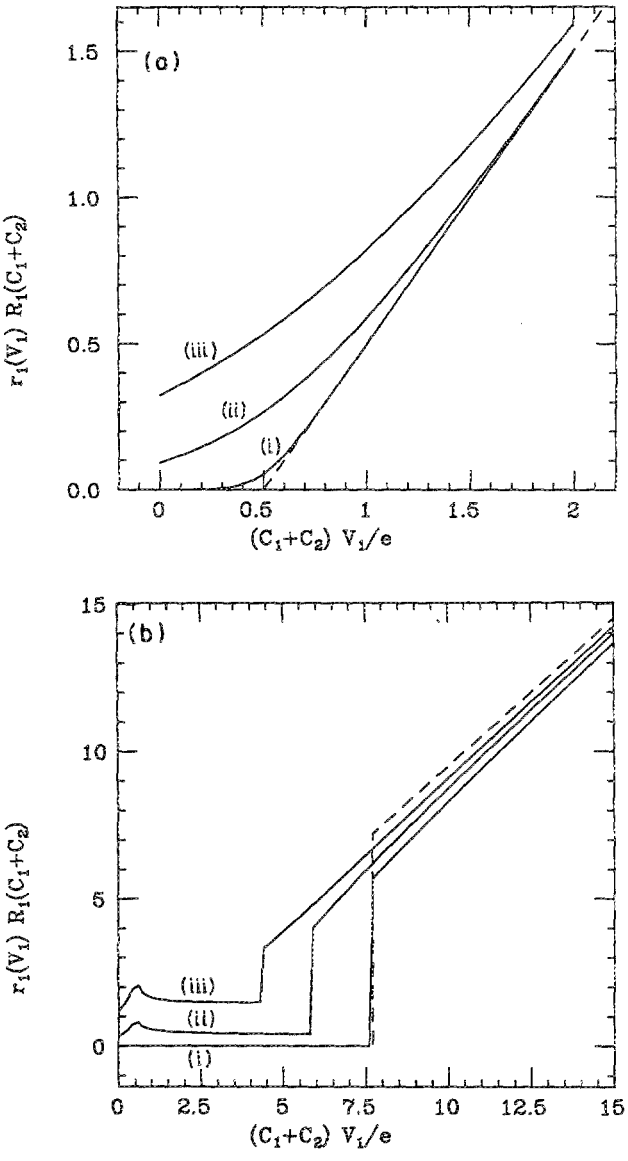

FIG. 2. (a) Numerically calculated electron tunneling rates for a normal-metal mesoscopic junction for different temperatures. The rate $l_1(V_1)$ is the reflection of $r_1(V_1)$ about the $V_1 = 0$ axis. The parameters are (i) $e^2/2(C_1 + C_2) = 20k_BT$, (ii) $e^2/2(C_1 + C_2) = 2k_BT$, and (iii) $e^2/2(C_1 + C_2) = k_BT$. The dashed line shows the form used in the calculations, given in Eq. 5. (b) Numerically calculated quasiparticle tunneling rates for a mesoscopic junction made from a superconducting material. The critical temperature is $T_c = 8$ K and $e^2/2(C_1 + C_2) = k_BT_c/4$. The parameters are (i) $T = 1$ K, (ii) $T = 4$ K, and (iii) $T = 6$ K. The dashed line shows the rate used in the calculations, given in (7).

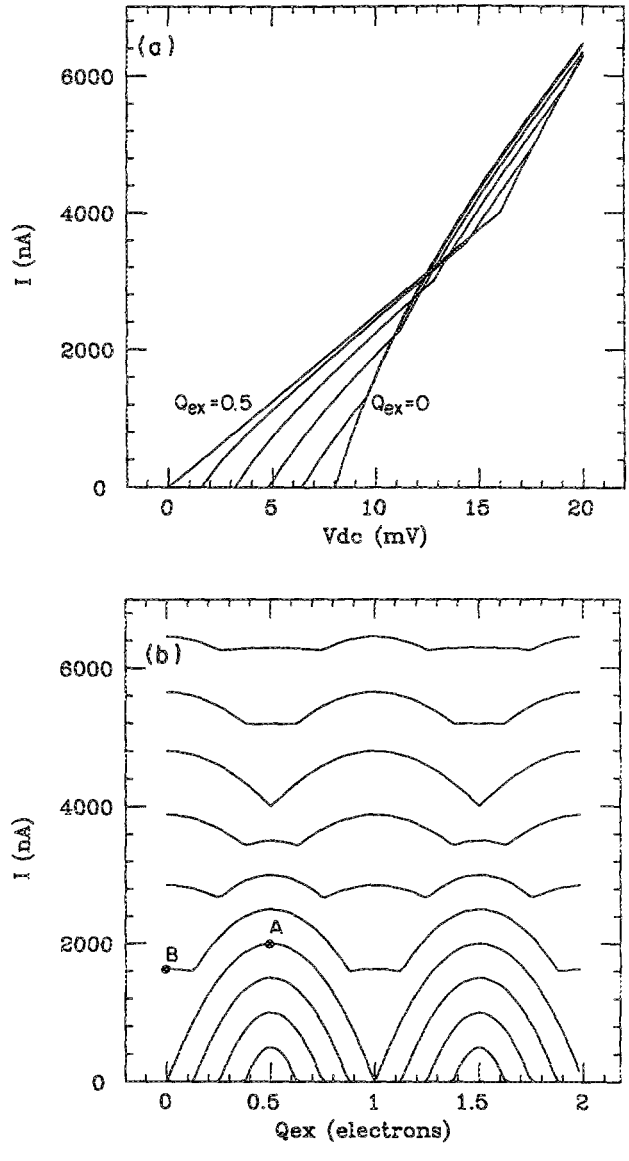

FIG. 3. (a) Calculated I-V_{dc} characteristics for the CHET circuit for various values of Q_{ex} when the tunnel junctions are identical and are made from normal metals. The parameters are $R_1 = R_2 = 1000\ \Omega$ and $C_1 = C_2 = 0.01$ fF, and Q_{ex} runs from 0 to 0.5 in steps of 0.1. (b) Calculated I-Q_{ex} characteristics for the same parameters as in (a) for various values of V_{dc}. The voltage V_{dc} runs from 2 to 20 mV in steps of 2 mV.

Coulomb blockade.[20] For $V_{dc} \lesssim e/C$, we see that as Q_{ex} increases this voltage offset decreases as the increased average charge in the interjunction region weakens the relative effect of the electrostatic charging barrier. This effect is periodic in Q_{ex}, since when $Q_{ex} = 1$, the added electron can simply tunnel out of the interjunction region, thereby reproducing the device state at $Q_{ex} = 0$. This periodicity is also present for larger voltages and is clearly shown in the I-Q_{ex} characteristics. For $V_{dc} \gg e/C$, we expect that the characteristics become independent of Q_{ex}. In this voltage range the average number of extra electrons between the two junctions is large so that variations on the order of Q_{ex} can no longer be observed. However, for the case of two identical junctions the effects of Q_{ex} wash out at lower voltages ($V_{dc} \gtrsim e/C$) because the probability distribution $\rho(N,t)$ is not well localized at a particular value of N. The variations of N help to wash out the effect of Q_{ex}.

In Fig. 4 the junction parameters have been chosen in order to make the tunneling rate of one junction much faster than the other (say $R_2C_2 \gg R_1C_1$). This condition yields clear steps in the I-V_{dc} characteristics.[20] The origin of these steps can be understood qualitatively by considering the shift in the voltage across each junction as a single electron tunnels across the first. Electrons tunnel across the first junction in response to the potential difference across it. The charge N can increase by one only when V_{dc} is raised by an amount

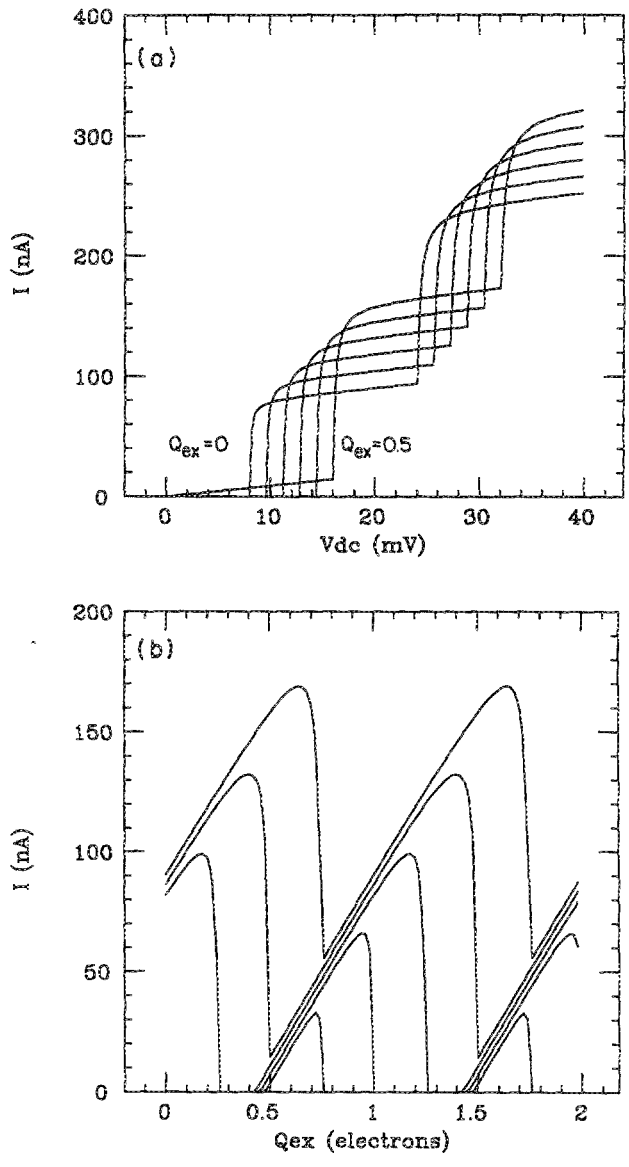

FIG. 4. (a) Calculated I-V_{dc} characteristics for the CHET circuit for various values of Q_{ex} when the tunnel junctions are made from normal metals and $R_2C_2 \gg R_1C_1$. The parameters are $R_1 = 1000\ \Omega$, $R_2 = 100\ \text{k}\Omega$, $C_1 = 0.001$ fF, and $C_2 = 0.01$ fF. The parameter Q_{ex} runs from 0 to 0.5 in steps of 0.1. (b) Calculated I-Q_{ex} characteristics for the same case as in (a) for various values of V_{dc}. The voltage V_{dc} runs from 4 to 20 mV in steps of 4 mV.

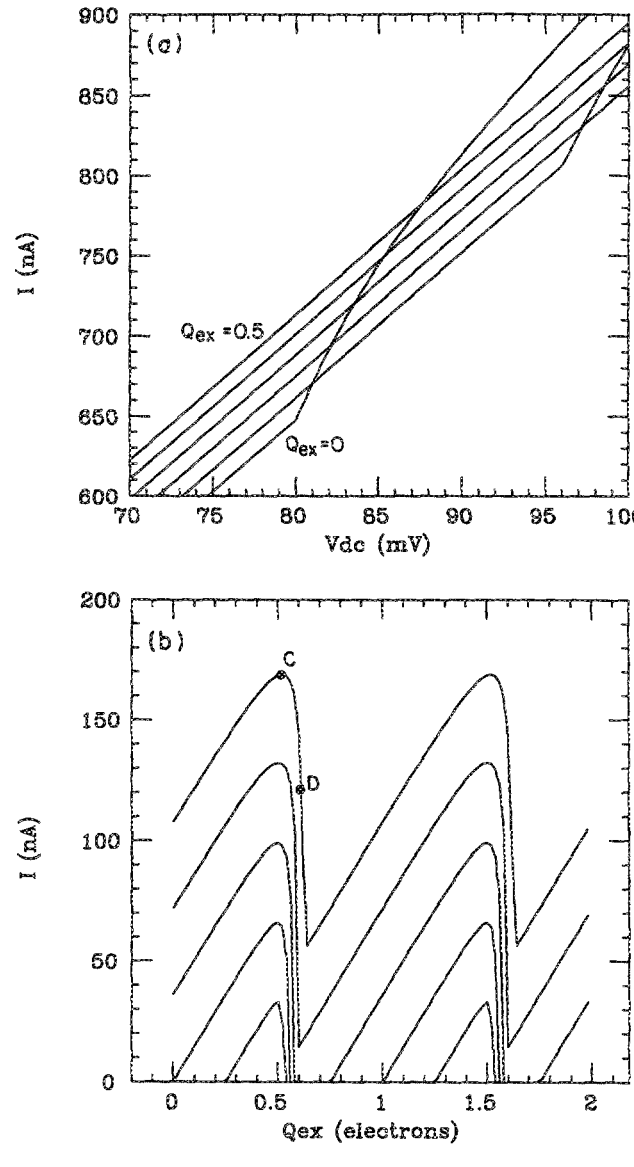

FIG. 5. (a) Calculated I-V_{dc} characteristics for the CHET circuit for various values of Q_{ex} when the tunnel junctions are made from normal metals and $R_2C_2 > R_1C_1$. The parameters are $R_1 = 1000\ \Omega$, $R_2 = 100\ \text{k}\Omega$, $C_1 = 0.01$ fF, and $C_2 = 0.001$ fF. The parameter Q_{ex} runs from 0 to 0.5 in steps of 0.1. (b) Calculated I-Q_{ex} characteristics for the same case as in (a). The voltage V_{dc} runs from 4 to 20 mV in steps of 4 mV.

sufficient to keep V_1 positive after the additional electron tunnels across. Since each additional electron shifts V_1 by an amount $e/(C_1 + C_2)$, the above requirement can be written as

$$\frac{C_2}{C_1 + C_2}\Delta V_{dc} = \frac{e}{C_1 + C_2}, \tag{11}$$

or

$$\Delta V_{dc} = e/C_2. \tag{12}$$

An external voltage increase of ΔV_{dc} increases N by one electron, producing a jump $\Delta V_2 = e/(C_1 + C_2)$ in the voltage across the second junction. This jump in V_2 increases the current by

$$\Delta I = \frac{\Delta V_2}{R_2} = \frac{e}{R_2(C_1 + C_2)}. \tag{13}$$

Similar arguments can be made when the voltage is applied in the opposite direction. These steps persist for large values of V_{dc}. In this case the second junction acts to hold charge in the interjunction region and therefore creates a well-localized $\rho(N,t)$ for a particular value of V_{dc}. Since $\rho(N,t)$ is well localized about a particular value of N, the effect of Q_{ex} is not washed out until $V_{dc} \gg e/C$.

The effect of Q_{ex} is to shift the I-V_{dc} curve up and to the right. The signal charge Q_{ex} simply increases the value of the extra interjunction electrons by a small amount, thereby shifting the points where the jumps in current occur. When $Q_{ex} = 1$, the I-V_{dc} curve shifts by a complete step and is

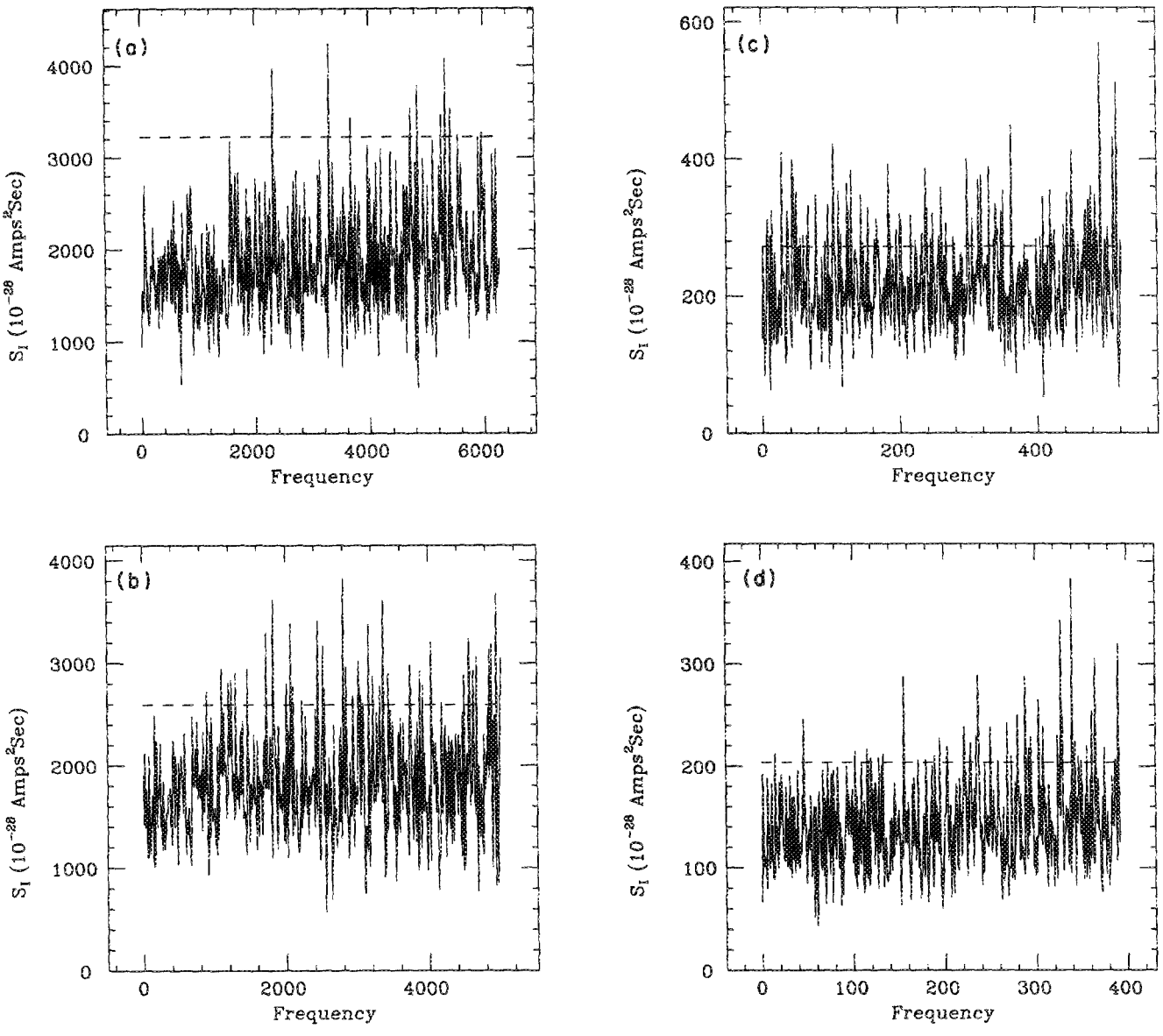

FIG. 6. Calculated power spectrum of the current noise for the CHET circuit when the junctions are identical and are made of normal metals. The time segment T is chosen such that ~ 6000 electrons pass through the CHET and τ_{max} is chosen to be $0.2T$. In all cases the horizontal line shows the current noise in a shot-noise device passing an identical current. (a) The parameters are $R_1 = R_2 = 1000\ \Omega$, $C_1 = C_2 = 0.01$ fF, $V_{dc} = 8$ mV, and $I_{ave} = 2000$ nA, corresponding to the point labeled *a* in Fig. 3(b). (b) The parameters are $R_1 = R_2 = 1000\ \Omega$, $C_1 = C_2 = 0.01$ fF, $V_{dc} = 10$ mV, and $I_{ave} = 1600$ nA, corresponding to the point labeled *b* in Fig. 3(b). (c) Calculated power spectrum of the current noise for the CHET circuit when the junctions are made from normal metals and $R_2C_2 > R_1C_1$. The parameters are $R_1 = 1000\ \Omega$, $R_2 = 100$ kΩ, $C_1 = 0.01$ fF, $C_2 = 0.001$ fF, $V_{dc} = 20$ mV, and $I_{ave} = 170$ nA, corresponding to the point *c* in Fig. 5(b). (d) Calculated power spectrum of the current noise for the CHET circuit when the junctions are made from normal metals and $R_2C_2 > R_1C_1$. The parameters are $R_1 = 1000\ \Omega$, $R_2 = 100$ kΩ, $C_1 = 0.01$ fF, $C_2 = 0.001$ fF, $V_{dc} = 20$ mV, and $I_{ave} = 127$ nA, corresponding to the point *d* in Fig. 5(b).

identical to the I-V_{dc} curve at $Q_{ex} = 0$. Again the periodic character is evident from the I-Q_{ex} characteristics.

In Fig. 5 we consider a third case, $R_1 < R_2$ and $C_1 > C_2$, in order to further demonstrate the variety of device characteristics attainable. The parameters are chosen such that junction No. 2 still acts to hold charge in the interjunction region, but not as effectively as the case for Fig. 4; thus the steps in the I-V_{dc} are not as pronounced. The distance between the steps is inversely proportional to C_2 and is therefore much greater in the present case. The I-V_{dc} curves are also primarily linear, excluding the points where the steps occur. Irrespective of the differences between the case of Fig. 5 and that of Fig. 4, the signal charge causes a similar effect, that of shifting the I-V_{dc} curve up and to the left.

For applications it is important to determine the noise level of the CHET circuit. Since the device current I is the desired output, we calculate the power spectrum of the current noise. The power spectrum of the current noise is given by

$$S_I(\omega) = \int_0^{\tau=\tau_{max}} \cos(\omega\tau) \times \frac{1}{T}\int_0^{t=T} [I(t)I(t+\tau) - I_{ave}^2]\,d\tau\,dt, \tag{14}$$

where T is the length of the time segment being analyzed, τ_{max} is the maximum correlation time considered, and I_{ave} is the average current over the period T. In Figs. 6(a)–6(d) we have calculated the current noise power spectrum for different circuit operating points. Figures 6(a) and 6(b) correspond to the operating points a and b shown in Fig. 3(b). Figures 6(c) and 6(d) correspond to the operating points c and d shown in Fig. 5(b). For comparison, the shot-noise level is indicated by a dashed line in each figure. This level is calculated by $S_{shot} = eI_{ave}$.[35] We note that the current noise level is comparable, but lower than, the shot-noise level for all the operating points chosen.

IV. SUPERCONDUCTING MATERIAL CHET

When the junctions of the CHET are made from superconducting materials, discontinuities in the device characteristics are expected as a result of the singularity in the density of states of the superconductor.[32,33] Also, the superconducting energy gap $\Delta(T)$ introduces a new energy scale into the problem. In Figs. 7(a)–7(c) we calculate the output current as a function of the applied signal charge for junctions made of superconducting materials. The three cases shown are those of $\Delta(T) < E_c$, $\Delta(T) \approx E_c$, and $\Delta(T) > E_c$, where $E_c = e^2/2(C_1 + C_2)$. For all three cases the junctions are identical. The effect of making the junctions from superconducting materials is to produce discontinuities in the I-Q_{ex} characteristics. This effect becomes more pronounced as $\Delta(T)$ becomes larger with respect to E_c. These discontinuities in the device current indicate a potential for fast transitions between device states necessary for switching applications. In Fig. 8 we show the I-V_{dc} characteristics for $\Delta \approx E_c$, again note the discontinuities in the characteristics.

V. DISCUSSION

Above we have shown the characteristics of a new device, the charge-effect transistor. This device can be made from normal metals and operates at temperatures below $T = e^2/2k_B C$, where $C^{-1} = C_1^{-1} + C_2^{-1}$. For junctions made from current lithographic techniques ($C \approx 0.1$ fF), this corresponds to a temperature of 10 K. For junctions with a capacitance of 10^{-18} F = 1 aF, this corresponds to a temperature of 1000 K. Such small capacitances have been claimed using a scanning tunneling microscope as a tunneling probe.[16] By fabricating junctions with capacitances on the order of 10 aF, it will be possible to operate such devices at room temperature. The nonlinearity in the I-V characteristic suggests many possible applications such as a switching element and a frequency mixer. If the junction is made from a superconducting material, then the discontinuity in the density of states enhances this nonlinearity. In a real experiment the observed I-V characteristics will be somewhat different from the ones presented here because of the finite response time of the voltage source. The semiclassical model as outlined in Sec. II assumes that the response time of the voltage source is instantaneous. A more detailed analysis is required to determine the dependence of the dynamics upon the time the electron takes while tunneling (τ_t), the relaxa-

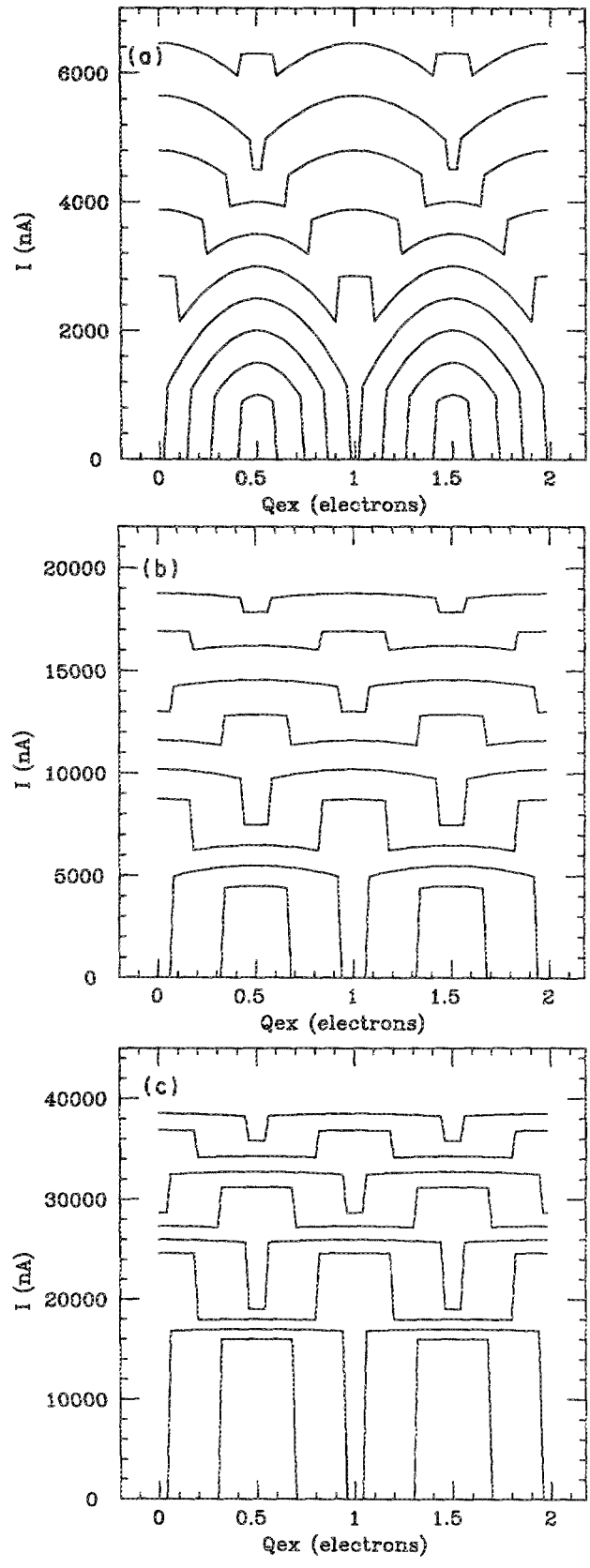

FIG. 7. Calculated I-Q_{ex} characteristics for the CHET circuit for various values of V_{dc} when the junctions are identical and are made from superconducting materials. The parameters are $R_1 = R_2 = 1000$ Ω, and $C_1 = C_2 = 0.01$ fF. The critical superconducting temperature T_c is varied between the figures to obtain different values of Δ. (a) $\Delta < E_c$, $T_c = 4$ K. The voltage V_{dc} runs from 4 to 20 mV in steps of 2 mV. (b) $\Delta \approx E_c$, $T_c = 25$ K. The voltage V_{dc} runs from 18 to 46 mV in steps of 4 mV. (c) $\Delta > E_c$, $T_c = 100$ K. The voltage V_{dc} runs from 64 to 92 mV in steps of 4 mV.

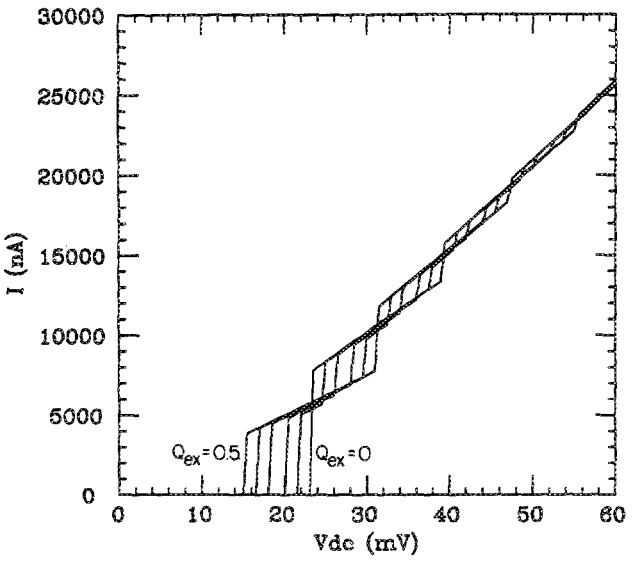

FIG. 8. Calculated I-V_{dc} characteristics for the CHET circuit for various values of Q_{ex} when the junctions are identical and are made from superconducting materials. The parameters are $R_1 = R_2 = 1000\ \Omega$, $C_1 = C_2 = 0.01$ fF, and $T_c = 25$ K. The parameter Q_{ex} runs from 0 to 0.5 in steps of 0.1.

tion time within the drop (τ_{in}), and the response time of the voltage source (τ_r).

A simple modification would be to make the junctions from a semiconducting material. This would introduce the semiconductor gap energy E_{gap} as a new energy scale in the problem. A second possible modification comes from making the central region so small that the density of states is discrete. By altering the bias voltage, it is possible to enhance or suppress tunneling to these discrete states.

ACKNOWLEDGMENTS

We have profited from many useful discussions with R. C. Jaklevic, Z. Schuss, and R. Wilkins. This research was partially supported by NSF Grant No. DMR 8608305 and Grant No. DAAL 03-87-k-0007 from the Army Research Office. M. A. is supported by a Regent's Fellowship from the State of Michigan, and K. M. is supported by a fellowship from the Center for High Frequency Microelectronics at the University of Michigan. E.B.-J. is a Bat-Sheva Fellow.

[1]B. R. Brewer, Ed., *Electron-Beam Lithography in Microelectronics Fabrication* (Academic, New York, 1980).
[2]For a review of mesoscopic systems, see Y. Imry, in *Memorial Volume in Honor of Professor Shang-Keng Ma*, edited by G. Grinstein and G. Mazenko (World Scientific, Singapore, 1986).
[3]E. Ben-Jacob and Y. Gefen, Phys. Lett. A **108**, 289 (1985).
[4]E. Ben-Jacob, Y. Gefen, K. Mullen, and Z. Schuss, in *SQUID 85*, edited by H. D. Hahlbohm and H. Lübbig (de Gruyter, Berlin, 1985).
[5]D. V. Averin and K. K. Likharev, in *SQUID 85*, edited by H. D. Hahlbohm and H. Lübbig (de Gruyter, Berlin, 1985).
[6]D. V. Averin and K. K. Likharev, Low Temp. Phys. **62**, 345 (1986).
[7]D. V. Averin and K. K. Likharev, Sov. Phys. JETP **63**, 427 (1986).
[8]F. Guinea and G. Schön, Europhys. Lett. **1**, 585 (1986).
[9]K. K. Likharev, IEEE Trans. Magn. **MAG-23**, 1138 (1987).
[10]D. V. Averin, Sov. J. Low Temp. Phys. **13**, 208 (1987).
[11]E. Ben-Jacob, Y. Gefen, K. Mullen, and Z. Schuss, Phys. Rev. B **37**, 7400 (1988).
[12]Y. Gefen and D. J. Thouless (unpublished).
[13]M. Büttiker, Phys. Rev. B **36**, 3548 (1987).
[14]K. K. Likharev (unpublished).
[15]K. Mullen, E. Ben-Jacob, and Y. Gefen, Physica B **152**, 172 (1988).
[16]U. Geigenmüller and G. Schön, Physica B **152**, 186 (1988).
[17]P. J. M. van Bentum, H. van Kempen, L.E.C. van de Leemput, and P. A. A. Teunissen, Phys. Rev. Lett. **60**, 369 (1988).
[18]M. Iansiti, A. T. Johnson, C. J. Lobb, and M. Tinkham, Phys. Rev. Lett. **60**, 2414 (1988).
[19]I. O. Kulik and R. I. Shechter, Sov. Phys. JETP **41**, 308 (1975).
[20]K. Mullen, E. Ben-Jacob, R. C. Jaklevic, and Z. Schuss, Phys. Rev. B **36**, 98 (1988).
[21]J. B. Barner and S. T. Ruggiero, Phys. Rev. Lett. **59**, 807 (1987).
[22]J. B. Barner and S. T. Ruggiero, Phys. Rev. B **36**, 8870 (1987).
[23]L. S. Kuz'min and K. K. Likharev, JETP Lett. **45**, 389 (1987).
[24]T. A. Fulton and G. J. Dolan, Phys. Rev. Lett. **59**, 109 (1987).
[25]P. J. M. van Bentum, R. T. M. Smokers, and H. van Kampen, Phys. Rev. Lett. **60**, 2543 (1988).
[26]V. Ambegaokar and A. Baratoff, Phys. Rev. Lett. **10**, 486 (1963); Phys. Rev. Lett. **11**, 104(E) (1963).
[27]K. Mullen and E. Ben-Jacob (unpublished).
[28]E. Ben-Jacob, K. Mullen, and G. Schön (unpublished).
[29]N. C. Van Kampen, *Stochastic Processes in Physics and Chemistry* (North-Holland, New York, 1981).
[30]T. L. Ho, Phys. Rev. Lett. **51**, 2060 (1983); E. Ben-Jacob, E. Mottola, and G. Schön, Phys. Rev. Lett. **51**, 2064 (1984).
[31]M. Tinkham, *Introduction to Superconductivity* (McGraw-Hill, New York, 1975).
[32]K. Mullen, E. Ben-Jacob, and Z. Schuss, Phys. Rev. Lett. **60**, 1097 (1988).
[33]K. Mullen, E. Ben-Jacob, and S. Ruggiero, Phys. Rev. B **38**, 5150 (1988).
[34]J. Bardeen, L. N. Cooper, and J. R. Schrieffer, Phys. Rev. **108**, 1175 (1957).
[35]S. O. Rice, Bell Syst. Tech. J. **23-24**, 282-332, 46-156 (1944, 1945), reprinted in *Noise and Stochastic Processes*, edited by N. Wax (Dover, New York, 1954).